Atmos. Chem. Phys. Discuss., 11, 11649–11690, 2011
www.atmos-chem-phys-discuss.net/11/11649/2011/
doi:10.5194/acpd-11-11649-2011

Atmospheric Chemistry and Physics Discussions

Climatology and trends in the forcing of the stratospheric zonal-mean flow

E. Monier[1] **and B. C. Weare**[2]

[1]Joint Program on the Science and Policy of Global Change, Massachusetts Institute of Technology, Cambridge, Massachusetts, USA
[2]Atmospheric Science Program, Department of Land, Air and Water Resources, University of California, Davis, California, USA

Received: 30 March 2011 – Accepted: 8 April 2011 – Published: 14 April 2011

Correspondence to: E. Monier (emonier@mit.edu)

Published by Copernicus Publications on behalf of the European Geosciences Union.

Abstract

The momentum budget of the Transformed Eulerian-Mean (TEM) equation is calculated using the European Centre for Medium-Range Weather Forecasts (ECMWF) Re-Analysis (ERA-40). This study outlines the considerable contribution of unresolved waves, dominated by gravity waves, to the forcing of the zonal-mean flow. A trend analysis, from 1980 to 2001, shows that the onset and break down of the Northern Hemisphere (NH) stratospheric polar night jet has a tendency to occur later. This temporal shift is associated with long-term changes in the planetary wave activity that are mainly due to synoptic waves. In the Southern Hemisphere (SH), the polar vortex shows a tendency to persist further into the SH summertime. This is associated with a statistically significant decrease in the intensity of the stationary EP flux divergence over the 1980–2001 period. Ozone depletion is well known for strengthening westerly winds through the thermal wind balance, which in turn causes a reduction in wave activity in high latitudes. This study suggests that the decrease in planetary wave activity provides an important feedback to the zonal wind as it delays the breakdown of the polar vortex. Finally, we identify long-term changes in the Brewer-Dobson circulation that, this study suggests, are largely caused by trends in the planetary wave activity during winter and by trends in the gravity wave forcing otherwise.

1 Introduction

Understanding stratospheric dynamics, its variability and interaction with photochemical processes has become increasingly important for the climate community. In the last decade, there has been growing evidence that the stratosphere can significantly influence the tropospheric weather and climate (Haynes, 2005; Baldwin et al., 2007). Baldwin and Dunkerton (2001) found that large circulation anomalies in the lower stratosphere precede tropospheric anomalies in the Arctic and North Atlantic Oscillations, and in the location of storm tracks. Therefore, understanding variations in the general

ACPD
11, 11649–11690, 2011

circulation of the stratosphere could provide additional tropospheric extended-range forecasting skills (Baldwin and Dunkerton, 2001; Kuroda, 2008). There are many theories describing how the stratosphere can impact the troposphere, such as the downward reflection of wave flux (Perlwitz and Harnik, 2003) or the downward control (Song and Robinson, 2004). Hartley et al. (1998) and Black (2002) have shown that any change in the potential vorticity (PV) in the lower stratosphere induces instantaneous changes in wind and temperature at the tropopause that lead to feedbacks on the troposphere. Also, several studies reveal that the Arctic Oscillation (AO) can propagate downward from the stratosphere to the troposphere (Baldwin and Dunkerton, 1999; Kuroda and Kodera, 1999, 2004; Limpasuvan et al., 2005). Finally, Ineson and Scaife (2009) show that the stratosphere plays a significant role in the European climate response to El Niño-Southern Oscillation (ENSO). For these reasons, a comprehensive understanding of the stratospheric dynamics variability and its causes is necessary in order to fully appreciate the potential impact of the stratosphere on climate change.

In addition, several studies have shown that the stratospheric dynamics have undergone significant changes in the last few decades. The Southern Hemisphere (SH) stratosphere exhibits a trend towards stronger westerly winds in the summer-fall season, producing a delay in the breakup of the polar vortex (Thompson and Solomon, 2002; Renwick, 2004). Karpetchko et al. (2005) show that wave forcing is not responsible for this long-term change and the trend is mainly attributed to Antarctic ozone depletion. As ozone loss in the polar region leads to an enhanced meridional temperature gradient near the subpolar stratosphere, it also results in the strengthening of westerly winds through thermal wind balance. Likewise, long-term trends in the Northern Hemisphere (NH) stratospheric dynamics have been identified. Hu and Tung (2003) detect a significant decline in wave activity in the higher latitudes, which starts from the early 1980s and exists only in late winter and springtime. This is consistent with the findings of Karpetchko and Nikulin (2004) who show a decrease in the vertical propagation of waves into the NH stratosphere in January and February. Additionally, Karpetchko and Nikulin (2004) reveal an increase in vertical propagation of waves in

ACPD
11, 11649–11690, 2011

November and December. A study of the long-term changes in stratospheric wave activity by Kanukhina et al. (2008) indicates an intensification in the stationary planetary wave number 1 activity in the lower stratosphere polar region over the last 40 years. Hu and Tung (2003) propose a similar mechanism as in the SH whereby ozone depletion induces stronger westerly winds which refract planetary waves toward low latitudes and cause the reduction in wave activity in high latitudes. However, Karpetchko and Nikulin (2004) do not find any statistically significant trend in the winter zonal winds. Thus, there is still a lot of uncertainty in the various trends seen in the stratospheric dynamics and the source and mechanism responsible for them.

The aim of this study is to investigate the role of the dynamical forcing in driving the stratospheric zonal-mean flow and its long-term changes, and in particular the dynamical response to long-term changes in stratospheric ozone. For this purpose, we perform a budget analysis of the Transformed-Eulerian Mean (TEM) formulation of the momentum equation with the European Centre for Medium-Range Weather Forecasts (ECMWF) Re-Analysis (ERA-40). The TEM formulation offers a useful diagnostic to interpret the forcing of the zonal-mean flow by eddies (Andrews et al., 1983). This work provides a deeper look into the contribution of planetary waves, their stationary and transient components, and gravity waves, to the forcing of the stratospheric zonal-mean zonal wind and the residual mean meridional circulation. Such analysis is vital as the impacts of ozone depletion and wave activity variability on the long-term changes in stratospheric dynamics are not yet fully understood. This paper is organized as follows. The data, the equations and the basic description of the various eddy flux terms involved in the TEM formulation are briefly introduced in Sect. 2. Section 3 describes the climatology of the stratospheric zonal-mean flow and its dynamical forcing, while Sect. 4 presents the results from the trend analysis of the momentum budget. Finally, the discussion and concluding remarks are presented in Sect. 5.

ACPD
11, 11649–11690, 2011

2 Data and methodology

2.1 Data

In this study, we use the six-hourly ERA-40 re-analysis (Uppala et al., 2005) in order to calculate the various terms involved in the Transformed Eulerian-Mean formulation of the momentum equation. The ERA-40 assimilates nearly all available data into a modern forecast model and provides a complete set of meteorological data, over the whole globe on a $2.5^{\circ} \times 2.5^{\circ}$ grid and over a long time period (1957–2001). Several studies have demonstrated the quality and usefulness of the ERA-40 data in the stratosphere. The annual cycle of the lower stratosphere in the ERA-40 compares well with other re-analysis datasets and the ERA-40 representation of the QBO is excellent up to 10 hPa (Pascoe et al., 2005). The monthly mean ERA-40 temperatures and zonal winds in the lower stratosphere compare well with the NCEP-National Center for Atmospheric Research (NCAR) reanalysis-1 after 1979 (Karpetchko et al., 2005). In addition, Knudsen et al. (2004) show that winter-averaged polar stratospheric cloud (PSC) areas in the NH, obtained from the ERA-40 and from the Free University of Berlin (FUB) analysis, which is largely independent of satellite data, agree well in most years. The ERA-40 dataset also shows several weaknesses, such as an enhanced Brewer-Dobson circulation (van Noije et al., 2004; Uppala et al., 2005) or vertically oscillating stratospheric temperature biases over the Arctic since 1998 and over the Antarctic during the whole period (Randel et al., 2004). Also, the ERA-40 re-analysis is unrealistic in the SH stratosphere during the pre-satellite era (Renwick, 2004; Karpetchko et al., 2005). Nonetheless, the ERA-40 re-analysis provides a reasonably reliable dataset in the lower stratosphere during the satellite era. For this reason, the climatological analysis of the wave forcing of the stratospheric zonal-mean flow is performed over the years 1980 to 2001, which coincides with the ozone depletion period, and for pressure levels up to 10 hPa.

ACPD
11, 11649–11690, 2011

E. Monier and B. C. Weare

2.2 Methodology

2.2.1 Transformed Eulerian-Mean formulation

This study uses the Transformed Eulerian-Mean (TEM) formulation of the momentum equation in log-pressure and spherical coordinates in order to accurately diagnose the eddy forcing of the stratospheric zonal-mean flow. In spherical geometry, the TEM zonal momentum equation is (based on Equation 3.5.2a from Andrews et al., 1987):

$$\underbrace{\frac{\partial \overline{u}}{\partial t}}_{\text{Momentum tendency}} = \underbrace{f\overline{v}^{\star}}_{\text{Coriolis force}} \underbrace{-\frac{\overline{v}^{\star}}{a\cos\phi}\frac{\partial}{\partial\phi}(\overline{u}\cos\phi) - \overline{w}^{\star}\overline{u}_z}_{\text{Advective terms}} + \underbrace{\frac{1}{\rho_0 a\cos\phi}\nabla\times F}_{\text{EP flux divergence}} + \underbrace{\overline{X}}_{\text{Residualterm}} \quad (1)$$

$$\underbrace{\frac{\partial \overline{u}}{\partial t}}_{\text{Momentum tendency}} = \underbrace{f\overline{v}^{\star}}_{\text{Coriolis force}} \underbrace{-\frac{\overline{v}^{\star}}{a\cos\phi}\frac{\partial}{\partial\phi}(\overline{u}\cos\phi) - \overline{w}^{\star}\overline{u}_z}_{\text{Advective terms}} + \underbrace{\frac{1}{\rho_0 a\cos\phi}\nabla\times F}_{\text{EP flux divergence}} + \underbrace{\overline{X}}_{\text{Residual term}} \quad (2)$$

In Eq. (2) and in the following equations, u is the zonal wind and the terms $\overline{v}^{\star}$, $\overline{w}^{\star}$ are, respectively, the horizontal and vertical components of the residual mean meridional circulation defined by (Eqs. 3.5.1a and b from Andrews et al., 1987):

$$\overline{v}^{\star} = \overline{v} - \frac{1}{\rho_0}\frac{\partial}{\partial z}\left(\rho_0 \frac{\overline{v'\theta'}}{\overline{\theta}_z}\right) \quad (3)$$

$$\overline{w}^{*} = \overline{w} + \frac{1}{a\cos\phi}\frac{\partial}{\partial\phi}\left(\cos\phi\frac{\overline{v'\theta'}}{\overline{\theta}_z}\right) \quad (4)$$

where the overbars and primes indicate respectively the zonal means and departures from the zonal mean. θ is the potential temperature, v is the meridional wind and w is the vertical wind. $\nabla \times \boldsymbol{F}$ is the divergence of the Eliassen-Palm (EP) flux vector and represents the divergence of the eddy heat and eddy momentum fluxes. The components of the EP flux vector $\boldsymbol{F}$ are defined by (Eqs. 3.5.3a and b from Andrews et al., 1987):

$$\boldsymbol{F}^{(\phi)} = \rho_0 a\cos\phi\left(\overline{u}_z\frac{\overline{v'\theta'}}{\overline{\theta}_z} - \overline{v'u'}\right) \quad (5)$$

$$\boldsymbol{F}^{(z)} = \rho_0 a\cos\phi\left[\left(f - \frac{1}{a\cos\phi}\frac{\partial}{\partial\phi}(\overline{u}\cos\phi)\right)\frac{\overline{v'\theta'}}{\overline{\theta}_z} - \overline{w'u'}\right] \quad (6)$$

Finally, $\overline{X}$ represents unspecified horizontal components or friction or other dissipative mechanical forcing (such as subgrid-scale gravity wave drag), and is calculated as the residual of the other terms.

Dunkerton (1978) showed that the B-D circulation should be interpreted as a Lagrangian mean circulation and could be approximated by the residual mean meridional circulation of the TEM equations. As a result, the residual mean meridional circulation is often used as a diagnostics for the B-D circulation (Callaghan and Salby, 2002; Nikulin and Karpechko, 2005; Miyazaki and Iwasaki, 2005; Eichelberger and Hartmann, 2005). Thus the various processes forcing the zonal-mean zonal momentum tendency that are investigated in this study are separated into four categories: the Coriolis force due to the B-D circulation, the advection of zonal-mean zonal momentum by the B-D circulation, the divergence of the EP flux or planetary wave forcing, and the residual term. Additionally, when we refer to the EP flux divergence, or $\nabla \times \boldsymbol{F}$, we

ACPD
11, 11649–11690, 2011

indicate the EP flux forcing term in Eq. (2), including the weight by the density, the Earth's radius and cosine of latitude. The signs shown in Eq. (2) are included in the various displayed terms. Each term is calculated using the six-hourly ERA-40 dataset and centered finite differences.

2.2.2 Stationary and transient components

Because stratospheric dynamics are primarily driven by planetary waves, whether directly or indirectly, it is useful to decompose the zonal momentum forcing into contributions from stationary and transient waves. Stationary planetary waves are excited by the orography (Charney and Eliassen, 1949), especially in the NH, as well as by land-sea heating contrasts, which vary on the seasonal time scale. Planetary transient waves, on the other hand, have smaller time scales ranging from a few days to a couple of weeks and dominate synoptic weather patterns. The stationary components are computed by averaging temperature and wind fields over a month and then calculating the various terms of the TEM formulation. Once the stationary component is removed from the total term, which is calculated every six hours, only the contribution from the transient waves is left (Madden and Labitzke, 1981).

3 Climatology of the stratospheric zonal-mean flow

3.1 Seasonal cycle of the zonal momentum budget

Figure 1 presents the annual cycle of the zonal-mean zonal wind, its tendency and forcing terms, averaged between 100 and 10 hPa for the 1980–2001 period. The annual cycle of the zonal flow shows distinct and well-known features such as the wintertime stratospheric polar night jets, strongest in the SH, and the latitudinal migration of the stratospheric tropical easterlies with the seasons (Oort, 1983; Andrews et al., 1987; McWilliams, 2006). In the NH, the maximum in the stratospheric polar vortex westerlies occurs from December to February and is centered on 60° N, while weak easterlies

ACPD
11, 11649–11690, 2011

are present from May to July. In the SH, the maximum in the westerlies occurs later in the winter than in the NH, from July to September, and is centered on 60° S. The zonal momentum tendency displays a clear seasonal cycle in the NH with an increase from July to December and a decrease from January to June with two distinct peaks (in the polar region and in the subtropics). In the SH, the momentum tendency presents a more complex structure with an increase lasting longer than in the NH, from January to August and a brief and intense decrease from September to December taking place mainly in the midlatitudes and polar region.

The Coriolis force due to the B-D circulation is characterized by an eastward forcing all year long except right along the Equator where its forcing is close to zero. The Coriolis force displays a pronounced seasonal cycle in the NH with a broad maximum in the midlatitudes from November to January and a minimum in June and July. In the SH, the Coriolis forcing presents two distinct peaks, weaker than in the NH, a brief and sharp maximum centered on 60° S from October to December and the other in the subtropics from May to July. Although much weaker than the other forcing terms, the advection of zonal momentum by the B-D circulation shows a clear seasonal annual cycle with the strongest forcing occurring in the wintertime. The advective terms correspond to a eastward forcing in the polar region and an westward forcing in the tropics in both SH and NH. The EP flux converges over most of the year and domain resulting in a continuous westward forcing, strongest in the midlatitudes and present in both hemispheres. A broad maximum in the EP-flux convergence is present from early winter until late spring in the NH and a sharp and brief peak is present in spring in the SH. Finally, the residual term contributes to a westward forcing during wintertime in the subtropics and polar regions.

The fact that the forcing of the stratospheric zonal wind takes place mainly in wintertime, particularly in the NH, is consistent with the finding of Charney and Drazin (1961) who showed that planetary Rossby waves can only propagate upward toward the stratosphere when the zonal wind is westerly but not too strong, which occurs in the wintertime in the NH. In the SH winter, the westerly winds are much stronger than

ACPD
11, 11649–11690, 2011

in the NH and as a result they inhibit the vertical propagation of planetary waves into the stratosphere. This leads to a delay in the forcing of the stratospheric zonal wind. The convergence of EP flux, which represents the westward force on the zonal-mean flow due to vertically propagating planetary waves breaking and dissipating into the stratosphere, is primarily responsible for the deceleration of the polar night jets. This deceleration is partially balanced by the Coriolis force due to the B-D circulation. While the advective terms have small magnitudes compared to the EP flux and Coriolis terms, they have the same magnitude as the zonal momentum tendency and thus cannot be entirely neglected. Finally, the residual term displays magnitudes similar to the EP flux term, particularly in the NH wintertime, and thus contributes to breaking down the polar night jets.

3.2 Vertical structure of the zonal momentum budget

An example of the vertical structure of the zonal-mean zonal wind, its tendency and forcing terms for the months of January-February-March (JFM) in the NH, when the polar vortex is breaking down, is presented in Fig. 2. The mean zonal winds exhibit strong westerlies in the subtropical lower stratosphere, corresponding to the top of the subtropical jet stream, and in the middle stratosphere over the subpolar region, where the stratospheric polar night jet is located. At the same time, the zonal momentum tendency shows a deceleration of the strong westerlies in the polar region, leading to the break down of the polar vortex. Figure 2 shows that the EP flux converges over the whole region leading to a deceleration of the zonal-mean zonal wind, strongest in the subtropical lower stratosphere and subpolar middle stratosphere. This deceleration is largely balanced by the Coriolis force. The relatively small impact of the advective terms is mainly confined to the middle stratosphere in the polar region and to the tropics below 70 hPa. Finally, the residual term presents a clear deceleration in the latitude band between 20° –40° N centered around 100 hPa with a maximum of around $2\,\mathrm{m\,s^{-1}\,day^{-1}}$. It also shows a strong deceleration in the middle stratosphere polar region which reaches $3\,\mathrm{m\,s^{-1}\,day^{-1}}$ above 10 hPa. The magnitudes of these values

ACPD
11, 11649–11690, 2011

confirm that the residual term plays a role in the momentum budget, thus it requires further interpretation.

3.3 Residual term

The residual term may be interpreted as friction and any wave forcing not included in the divergence of the EP flux, such as gravity wave drag or other unresolved processes. In the ERA-40 model, the influence of subgrid-scale orography on the momentum of the atmosphere is represented by a combination of lower-troposphere drag created by orography, and of vertical profiles of drag due to the absorption and reflection of vertically propagating gravity waves generated by stably stratified flow over the subgrid-scale orography Lott and Miller (1997). Several studies have estimated the stratospheric gravity wave drag as the residual term from the momentum equation (Hartmann, 1976; Hamilton, 1983; Smith and Lyjak, 1985; Alexander and Rosenlof, 1996, 2003). Alexander and Rosenlof (2003) estimates the gravity-wave driven forcing in the stratosphere from November 1991 to June 1997 as the residual from the TEM equations using data from the Upper Atmosphere Research Satellite (UARS) and the UK Met Office (UKMO). They show that with some averaging of the gravity wave drag estimates, the seasonal cycles are robust, and the magnitudes are reliable within approximately a factor of 2.

Figure 3 shows the height-latitude profiles of the residual term over both hemispheres for the winter and summer seasons. The residual term is large during winter and generally negative while it is noisier during summer, mainly because all the terms in the TEM equations are small. In the NH winter, the local maximum located just above the subtropical jet stream near 100 hPa and between 30°–40° N, with decelerations of 2 m s^{-1} day^{-1}, is in agreement with previous analysis and modeling studies (Palmer et al., 1986; Scinocca and McFarlane, 2000; McFarlane, 2000) and radar measurements (Fritts and Alexander, 2003). The second local maximum, in the middle to upper stratosphere in the polar region with decelerations greater than 3 m s^{-1} day^{-1} above 10 hPa, is within the range of gravity wave drags parameterized in modeling studies

ACPD
11, 11649–11690, 2011

(Smith and Lyjak, 1985; Scinocca and McFarlane, 2000; McFarlane, 2000; Mieth et al., 2004; Richter et al., 2008). In the SH winter, the subtropical maximum is weaker than in the NH, primarily because of the comparative lack of topography. Also the decelerations in the polar region extend further into the lower stratosphere, in agreement with Scinocca and McFarlane (2000). While there is some disparity between the various gravity wave drag parameterizations, the residual term of the TEM equation is consistent with the major characteristics of a gravity wave drag.

Focusing on the tropics, Fig. 4 shows the residual term and zonal-mean zonal wind averaged over the equatorial latitude band 30° S–40° N as a function of height and time. Tongues of eastward acceleration from the residual term descend in time and lead the eastward wind phase of the Quasi Biennial Oscillation (QBO) by about 3 to 5 months. Similarly, a deceleration by the residual term occurs during the descent of the westward QBO phase. As such, the residual term is consistent with the tropical gravity wave forcing of the QBO and is comparable to numerous analyses and global model studies (Dunkerton, 1997; Scaife et al., 2002; Alexander and Rosenlof, 2003). Finally, an analysis of the seasonal cycle of the tropical residual term (not shown) reveals a migration of its maximum with latitudes across the Equator between boreal and austral summers, following the Inter-Tropical Convergence Zone (ITCZ). The 22-year mean residual term exhibits positive values in winter and summer, which correspond to a deceleration of the zonal-mean zonal wind since the prevailing winds are easterly in the tropical region. In January, the drag force is located south of the Equator and reaches 0.4 $m\,s^{-1}\,day^{-1}$ above 100 hPa while it is located north of the Equator in July and shows stronger accelerations, reaching up to 0.5 $m\,s^{-1}\,day^{-1}$. This result is in agreement with Chun et al. (2004) who introduces a parameterization scheme of gravity wave drag induced by cumulus convection in the National Center for Atmospheric Research Community Climate Model (NCAR CCM3).

The uncertainties in the residual term in this analysis are difficult to quantify, partly because there are no global observations of gravity wave drag. Notably, there exists considerable discrepancy in the representation of the B-D circulation among the

ACPD
11, 11649–11690, 2011

E. Monier and B. C. Weare

various reanalyses currently available, especially in low latitudes (Randel et al., 2008; Iwasaki et al., 2009). So while it is valid to use the ERA-40 re-analysis for the demonstration of the method, the results might be dependent on the biases and should eventually be compared to results from other datasets. Nonetheless, the seasonal cycle and magnitudes of the residual term are indeed consistent with gravity wave drags used in various studies. As a simple test of the possible influence of the known overestimate of the B-D circulation in the ERA-40 reanalysis, we recalculated the budget assuming a decrease in $\overline{v}^{\star}$ and $\overline{w}^{\star}$ of 25%. The resultant figures, comparable to Fig. 3, are qualitatively nearly identical with slight decreases in magnitude of less than 20%. Furthermore, the estimation of unresolved processes as the residual term in the TEM momentum equation is likely to be an improvement over many studies where the effects of unresolved waves are crudely parameterized using a simple Rayleigh friction coefficient (Schoeberl and Strobel, 1978; Holton and Wehrbein, 1980; McLandress, 1998; Seol and Yamazaki, 1999), thus assuming a deceleration linear to the mean zonal wind. Shepherd and Shaw (2004) suggest that a Rayleigh friction introduces a nonphysical momentum sink and Haynes (2005) finds it difficult to argue that such a friction is at all relevant in the stratosphere.

3.4 EP flux divergence

While the residual term seems to contribute to the momentum budget in specific regions of the stratosphere, the main forcing in the deceleration of the zonal wind in the NH wintertime is the EP flux divergence. An example of the vertical structure of the EP flux vector, the EP flux divergence and its horizontal and vertical components for JFM is shown in Fig. 5. A distinct property of the EP flux divergence is the competition between its two components, which largely cancel each other in the extratropics. $\nabla \times \boldsymbol{F}^{(\phi)}$ is dominated by the horizontal divergence of the meridional eddy momentum flux and $\nabla \times \boldsymbol{F}^{(z)}$ is controlled by the vertical divergence of the meridional eddy heat flux (Andrews et al., 1987). Figure 5 underlines the fact that while the eddy momentum flux and eddy heat flux have contributions of opposite sign, they do not act separately but

ACPD
11, 11649–11690, 2011

in combination, with a net impact resulting in a westward body force that decelerates the polar vortex in the NH wintertime. In addition, the presence of a greater land area and topography distribution in the NH results in a stronger contribution from stationary processes, which are forced by topography and land-sea heating contrasts. However, the transient contribution is not negligible. The main difference between the stationary and transient components resides in the presence of a distinct divergence of the transient EP flux in the polar region middle stratosphere. While considerable divergence of EP flux can happen during sudden stratospheric warming events (Palmer, 1981), it is unclear why it is not removed from the climatology mean.

Under the WKBJ (Wentzel-Kramers-Brillouin-Jeffreys) approximation and when dealing with planetary waves with small latitudinal and vertical wavelength, it can be shown that the EP flux vector is proportional to the local group velocity projected onto the meridional plane (Edmon Jr et al., 1980). Thus, $\boldsymbol{F}$ is a useful diagnostic tool for the net propagation of wave energy by planetary waves from one region, at one latitude and one height, to another. Figure 5 indicates that, in the NH wintertime, the vertical component of the EP flux vector, dominated by the meridional eddy heat flux, is oriented upward and decreases with height, leading to a net convergence. Concurrently, the horizontal component of the EP flux vector shows that planetary waves propagating into the stratosphere are bent away from the stratospheric polar night jet toward the Equator at midlatitudes and toward the pole in the lower stratosphere polar region. This leads to a strong divergence of the meridional eddy momentum flux superposed onto the location of the strong westerlies. Consequently, the cancellation between the components of the EP flux divergence is the result of the refraction of planetary waves around the stratospheric polar night jet. Indeed, the effective index of refraction for the planetary waves depends primarily on the distribution of the zonal mean wind with height and energy can be refracted in regions where the zonal wind is westerly and large, like the stratospheric polar night jet (Charney and Drazin, 1961).

A similar analysis of the EP flux terms for the SH reveals that the main difference between the two hemispheres is the stronger contribution of transient wave forcing.

ACPD
11, 11649–11690, 2011

Trends in forcing of stratospheric zonal-mean flow

E. Monier and B. C. Weare

The contribution of stationary processes is mostly limited to the polar region, where the presence of the asymmetric Antarctic topography and ice-sea heating contrasts drives stationary wave activity (Parish et al., 1994; Lachlan-Cope et al., 2001). Overall, the analysis of the EP flux shows that both stationary and transient planetary waves contribute to the propagation of wave energy into the stratosphere. It also suggests a complex interplay between the eddy momentum and eddy heat fluxes in the stratosphere in the overall driving of the zonal-mean zonal wind.

3.5 Correlations of zonal momentum forcing

To gain more insight into the relative contributions of the forcing terms to the zonal wind variability, spatial correlation coefficients between the forcing terms are calculated and shown in Fig. 6. This analysis is similar to the statistics presented in Pfeffer (1992), but is extended to a 22-year daily climatology and includes an analysis of the stratosphere. It also focuses on one hemisphere at a time to account for the strong seasonality of the wave-mean flow interaction in the stratosphere. In the stratosphere, the correlation coefficients present a strong seasonality due to the absence of planetary wave propagation into the stratosphere at midlatitudes in summer. Figure 6 reveals that, contrary to the troposphere where the zonal momentum tendency is highly correlated with $\nabla \times \boldsymbol{F}^{(\phi)}$ but not with $\nabla \times \boldsymbol{F}^{(z)}$, the zonal momentum in the stratosphere is better correlated with the divergence of the EP flux than with either of the contributions from its separate components. This confirms that the eddy momentum and eddy heat fluxes in the stratosphere act in combination to force the zonal-mean zonal wind. The correlations between the momentum tendency and the EP flux divergence are strongest in March in the NH stratosphere, where they reach 0.5. Meanwhile, the momentum tendency is highly correlated with the sum of the Coriolis, advective and residual terms in the summertime, with correlations above 0.7, but not with each individual terms. Also, the Coriolis and advective terms in the troposphere exhibit a high negative correlation with $\nabla \times \boldsymbol{F}^{(z)}$, reflecting the fact that the wave drag exerted by $\nabla \times \boldsymbol{F}^{(z)}$ is consumed by driving the B-D circulation. However, in the stratosphere, the Coriolis and advective terms are poorly correlated with $\nabla \times \boldsymbol{F}^{(z)}$ or even $\nabla \times \boldsymbol{F}$, with a maximum correlation near 0.4 during winter. Instead they show a high negative correlation with the residual term, reaching a maximum of 0.9 from spring to fall when the EP flux divergence is weak. This suggests that in the Northern Hemisphere, unresolved forces, such as subgrid-scale gravity waves, contribute substantially to driving the B-D circulation. The same analysis was done for the Southern Hemisphere and yields similar results.

It is important to note that the B-D circulation is a non local response to wave driving and that downward control implies that the vertical velocities at a specific level are controlled exclusively by the wave forcing above that level (Haynes et al., 1991). This is likely to affect the physical significance of the correlations between the Coriolis and advective terms and the wave forcing terms. Furthermore, the uncertainties in the residual term due to the B-D circulation bias in the ERA-40 can contribute to the strong anti-correlation between the residual term and the Coriolis and advective terms. Nonetheless, the significant contribution of gravity waves in driving the B-D circulation has been evidenced in several studies based on the analysis of climate-chemistry model simulations (Li et al., 2008; McLandress and Shepherd, 2009; Butchart et al., 2010). This study only confirms the substantial influence of subgrid-scale processes in driving stratospheric dynamics.

4 Trends in the wave forcing of the stratospheric zonal-mean momentum

4.1 Zonal-mean zonal wind

The long-term trends and interannual variability of the lower and middle stratosphere zonal-mean zonal wind are investigated in Fig. 7. The variances and trends are calculated after the zonal-mean zonal wind is averaged between 100 and 10 hPa. In the tropics, the zonal wind displays a large variance representing a strong interannual variability all year long, which corresponds to the Quasi-Biennial Oscillation (QBO). The tropical variability shows a maximum in variance during the NH late spring, which is

ACPD
11, 11649–11690, 2011

E. Monier and B. C. Weare

consistent with the fact that the onset of both easterly and westerly QBO phases occurs mainly during NH late spring at the 50 hPa level (Dunkerton, 1990; Baldwin et al., 2001). Since the period of the QBO is variable and because the duration of each phase at any level is long compared with the transition time, the strongest variability tends to occur near the phase transition. Outside the tropics, the zonal wind variance is large in the polar region from early winter until early spring in the NH and limited to the late spring in the SH, which is likely associated with the breakdown of the polar vortex. The trend analysis reveals a long-term increase in the SH zonal wind from November to January, which is only statistically significant in December and January. This indicates that the SH polar vortex tends to persist longer into the summer, towards the end of the analysis period. In particular, the SH zonal wind has increased in December at a rate of $3.5\,\mathrm{m\,s^{-1}}$ per decade and at a 99% significance level (calculated using a two-tailed Student's *t*-test). This result is in agreement with several studies (Thompson and Wallace, 2000; Thompson and Solomon, 2002; Renwick, 2004; Karpetchko et al., 2005). Several of the later years (1998, 1999 and 2001) display strong westerlies close to $10\,\mathrm{m\,s^{-1}}$ in December, compared to the 22-year mean that is close to zero. In the NH, negative trends in the zonal wind are present in the late fall and early winter. However, these negative trends are only statistically significant in December, when the zonal wind has weakened at a rate of over $4\,\mathrm{m\,s^{-1}}$ per decade, with a 95% statistical significance level. Meanwhile, positive trends occur from February to March, during the breakdown of the polar vortex, however they are not statistically significant. For example, the March westerlies have strengthened, at a rate close to $3\,\mathrm{m\,s^{-1}}$ per decade, with a 87% significance level. While that trend shows only a moderate statistical significance in this analysis, it is similar to results by Thompson and Wallace (2000) who show that the westerlies near 55° N have increased by as much as $10\,\mathrm{m\,s^{-1}}$ over 30 years (1968-1997) at 50 hPa. Overall, the trends in the NH zonal-mean zonal winds indicate a temporal shift in the timing of the NH polar vortex that seems to be pushed further into the wintertime.

ACPD
11, 11649–11690, 2011

4.2 Wave forcing of zonal momentum budget

Figure 8 shows the annual cycle of the linear trends of the momentum tendency and its forcing terms over 1980–2001 in the polar regions. In the NH, positive trends in the Coriolis and advective terms are present from spring to fall and are largely balanced by opposite trends in the residual term. These trends are statistically significant in April and May, and from August to September. An analysis of the residual mean meridional mass stream function (not shown) shows that the positive trends in the Coriolis and advective terms are associated with an intensification of the B-D circulation. In winter, the Coriolis and advective terms experience negative trends that are offset by positive trends in the EP flux divergence (i.e. decrease in the convergence of EP flux), though not statistically significant at the 95% confidence level. However, Hu and Tung (2003) find a statistically significant reduction in planetary wave activity in the NH high latitudes (50° –90° N) in late winter and early spring (JFM) in the NCEP-NCAR-reanalysis. The lack of statistical significance in this study is possibly due to the large averaging area (100 to 10 hPa and 50° –70°) so that further analysis without the averaging is necessary to determine whether the trends in the planetary wave activity are real or not. Overall, the long-term trends in the B-D circulation in the NH are consistent with the response to a doubled CO_2 climate found in several studies (Eichelberger and Hartmann, 2005; Butchart et al., 2006; Haklander et al., 2008). This analysis suggests that the intensification of the B-D circulation from spring to fall is largely driven by trends in the residual term while the decrease in winter is driven by trends in the planetary wave forcing. This finding is also consistent with previous studies based on climate-chemistry model simulations (Li et al., 2008; McLandress and Shepherd, 2009; Butchart et al., 2010) that find the role of gravity wave drag in driving long-term changes in the B-D circulation significant. Also, Li et al. (2008) find that the long-term changes in the B-D circulation in the polar stratosphere are season and hemisphere dependent, confirming the necessity to investigate the seasonality of trends. The impact of the combined trends of the various forcing terms can be seen in the trends of the zonal momentum tendency.

ACPD
11, 11649–11690, 2011

In particular, the negative trend in the December zonal winds in Fig. 7 is preceded by a negative trend in the zonal momentum tendency in November, which is accompanied by a trend in the EP flux divergence. Similarly, the positive trend in the polar region zonal-mean zonal wind in March is preceded by a positive trend in the zonal momentum tendency in January and February, which is associated with a trend in the EP flux divergence.

In the SH, the Coriolis and advective terms exhibit positive trends in summer and fall and negative trends at other times, associated with changes in the B-D circulation. Like in the NH, these long-term changes are largely balanced by trends of opposite signs in the residual term, except in November and December when the trends in the EP flux divergence are large and drive changes in the B-D circulation. This further underlines the intricate role of unresolved processes, especially gravity waves, in driving long-term changes in the B-D circulation. In November, the convergence of EP flux that is responsible for the breakdown of the polar vortex has weakened over the 1980–2001 period at a rate of $0.46\,\mathrm{m\,s^{-1}\,day^{-1}}$ per decade, statistically significant at the 97.5% confidence level. Meanwhile, the convergence of EP flux has intensified in December at a rate of $0.38\,\mathrm{m\,s^{-1}\,day^{-1}}$ per decade, statistically significant at the 99% level. This indicates a temporal shift in the strength of the planetary wave forcing from November to December in SH polar region. Contrary to the NH, the zonal momentum tendency displays statistically significant trends in November and December concurrent to the trends in the planetary wave forcing. Because the 22-year mean zonal momentum is negative in November, the positive trend corresponds to a long-term weakening of the deceleration of polar vortex and explains the persistence of the polar vortex into the summer that was discussed previously.

Overall, Fig. 8 underlines the significant role of the residual term, dominated by gravity waves, in driving long-term changes in the B-D circulation during seasons when the planetary wave activity is weak. This analysis also shows that trends in the polar region zonal-mean zonal winds are preceded by trends in the momentum tendency and in the planetary wave forcing, with a lag of one month. This is particularly obvious in

ACPD
11, 11649–11690, 2011

Trends in forcing of stratospheric zonal-mean flow

E. Monier and B. C. Weare

November and December in the SH.

The vertical structure of the trends in the EP flux vector and its divergence in the SH for the month of November is shown in Fig. 9. It indicates a strong and significant decrease in the convergence of EP flux in the polar region between 100 and 10 Pa, statistically significant at the 95% confidence level. The decrease in planetary wave activity is mainly associated with stationary waves, though the statistical significance of the trends in the stationary EP flux divergence is weak. Figure 9 also shows that there is no significant trend associated with transient wave activity. The analysis of the trends in the EP flux vector demonstrates that significantly less energy is being transported vertically into the stratospheric polar region by planetary waves, especially by stationary waves. Meanwhile, trends in the horizontal component of the EP flux are weak and not significant. A similar analysis is done for the month of February in the NH and shown in Fig. 10. A significant decrease in the strength of the EP flux divergence is present in the subpolar and polar region below 100 hPa and above 20 hPa with competing contribution from stationary (intensification) and transient (weakening) waves. Overall, the trend analysis of the EP flux divergence is noisy and does not paint a clear picture. However, the EP flux vector exhibits more distinct patterns. Significantly less energy is transported vertically into the stratosphere by transient waves in the later years. Meanwhile a positive trend in the vertical component of the stationary EP flux vector is present between 50°–60°, consistent with the findings of Kanukhina et al. (2008), but this trend is not statistically significant. Moreover, this analysis shows a significant tendency toward more poleward refraction of stationary waves in the polar region and of transient waves at mid-latitudes. The study of the trends in the NH EP flux forcing for the month of November (not shown) reveals an increase in wave activity, which is statistically significant at midlatitudes and at several pressure levels in the polar region. This increase is principally due to transient waves propagating from the troposphere into the stratosphere significantly more in the later years. Concurrently, the equatorward refraction of planetary waves is greatly increased. In general, long-term changes in the planetary wave activity in the NH polar region are associated

ACPD
11, 11649–11690, 2011

with transient waves, a finding in agreement with McLandress and Shepherd (2009). Meanwhile, the trends in the EP flux in the SH are largely due to changes in stationary waves. Besides, the systematic analysis of trends in the EP flux vector and its divergence reveals tendencies consistent with that of the polar night jet. In the SH, a significant decrease in the planetary wave activity occurs in November, one month before the strongest and most significant positive trend in the zonal-mean zonal wind that corresponds to a delay in the breakdown of the polar vortex.

5 Conclusions

An analysis of the budget of the TEM momentum equation in the ERA-40 re-analysis provides further insight into the role of the planetary and gravity wave forcing on the stratospheric zonal-mean flow. The resolved terms in the momentum equation are the zonal momentum tendency, the Coriolis force and advective terms due to the B-D circulation, and the Eliassen-Palm flux divergence, which is a measure of the planetary wave forcing. In addition, a residual term is calculated from the other terms in the TEM momentum equation. The climatology of the resolved forcing terms is consistent with the wave-mean flow interaction theory, as the EP flux divergence contributes to the breakdown of the polar vortex while being balanced by the Coriolis force due to the B-D circulation. Meanwhile, the residual term displays many of the characteristic features of a gravity wave drag, including location, seasonality and magnitude compared to model simulations and measurements (Palmer et al., 1986; Dunkerton, 1997; Scinocca and McFarlane, 2000; McFarlane, 2000; Scaife et al., 2002; Fritts and Alexander, 2003) and was identified as a gravity wave drag in numerous studies (Hartmann, 1976; Hamilton, 1983; Smith and Lyjak, 1985; Alexander and Rosenlof, 1996, 2003). As a result, the momentum budget based on the TEM framework presented in this study provides a reasonable method to investigate the dynamical forcing in the stratosphere over the whole globe and over long time periods using re-analysis datasets. The momentum

ACPD
11, 11649–11690, 2011

budget outlines the significant contribution of the residual term in driving the stratospheric circulation, as it exhibits magnitudes similar to that of the EP flux divergence in some regions of the stratosphere. In fact, gravity waves may play an equally large role as planetary waves in driving the B-D circulation, especially during spring, summer and fall. The correlation analysis in Fig. 6 further highlights the differences between the balances in the momentum budget in the troposphere and stratosphere.

The trend analysis shows that there is a statistically significant weakening of the Northern Hemisphere stratospheric polar night jet in December and a moderately significant strengthening in March, hinting at a delay of the breakdown of the polar vortex. Both changes in the strength of the westerly winds follow changes in the planetary wave activity, mainly due to transient waves, with a delay of one month. This is consistent with the findings of Karpetchko and Nikulin (2004) who observed a decrease in the heat flux in January and February in the NCEP-NCAR-reanalysis. In their study, Karpetchko and Nikulin (2004) fail to link the trend in the wave activity to changes in the zonal-mean zonal wind because they only investigate trends in the polar night jet at the same period, and not a month later. This underlines the importance of a complete analysis of the seasonality of the long-term changes in the stratospheric dynamics. In the Southern Hemisphere, the polar vortex also shows a tendency to persist further into the SH summertime. This is associated with a statistically significant decrease in the intensity of the stationary EP flux divergence. Thus, the two hemispheres differ in the source of the decrease in wave activity: transient waves in the NH and stationary waves in the SH.

Several studies have attributed the ultimate cause of the delay in the breakdown of the SH polar vortex to ozone depletion (Thompson and Solomon, 2002; Renwick, 2004). Weare (2009) showed that there is a distinct symmetric mode between the zonal wind and ozone in the SH and that this mode contains a clear long-term trend. Hu and Tung (2003) advance a mechanism whereby ozone depletion leads to an enhanced meridional temperature gradient near the subpolar stratosphere, strengthening westerly winds. The strengthened winds would then refract planetary waves toward low

ACPD
11, 11649–11690, 2011

latitudes and cause the reduction in wave activity in high latitudes. It is also possible that the ozone depletion directly impacts the vertical propagation of planetary waves and in turn the zonal wind, as suggested by the ozone-modified refractive index for vertically propagating planetary waves introduced by Nathan and Cordero (2007), which accounts for how ozone photochemistry, ozone transport, and Newtonian cooling can combine to modify wave propagation and drag on the zonal-mean flow. There is no doubt that ozone changes result in changes in the strength of the zonal wind, especially in the SH where ozone depletion is very large. However, the strongest ozone trends over Antarctica take place from September to November in the ERA-40 (Monier and Weare, 2011), while the statistically significant long-term changes in the zonal wind are limited to the months of December and January. This indicates a delay of two months in the dynamical response to ozone depletion in the SH. This analysis suggests that the absence of any significant trends in the zonal wind in September and October is due to the absence of eddy feedback. During these months, the planetary wave activity is weak because the strength of the polar vortex suppresses the vertical propagation of planetary waves into the stratosphere. Meanwhile, in November when the polar vortex begins to break down, the vertically propagating waves can be modulated by the strength of the westerlies (associated with ozone depletion) and provide a strong positive feedback to the strength of the zonal-mean zonal wind. Furthermore, the significant increase in the planetary wave activity in the SH in December is most likely related to the delayed breakup of the polar vortex: as the transition to easterlies in the stratosphere occurs later in the season, the stratosphere can still support wave propagation, resulting in an increased propagation in December. In the NH, the planetary wave forcing is sustained from fall until late spring, and the timing of the strongest ozone depletion coincides with the break down of the polar vortex, in March (Monier and Weare, 2011). As a result, there is no delay between the ozone trends and the response of the zonal winds. As such, this analysis underlines the important role of planetary wave feedback in the dynamical response of the stratosphere to ozone changes. This study also suggests that the decrease in planetary wave activity associated with the sustained polar vortex is primarily due to a reduction in the vertical propagation of planetary waves. The changes in the meridional propagation of planetary waves are not statistically significant in the SH while they lead to more refraction toward the pole in the NH.

Finally, long-term changes in the residual mean meridional circulation were found in both hemispheres. In the NH, the B-D circulation significantly intensifies from spring to fall as a result of an increasing gravity wave drag. In winter, the strength of the residual circulation weakens due to a decrease in the planetary wave activity. Meanwhile, the residual mean meridional circulation intensifies in the SH during summer and fall and weakens during winter and spring. These trends are driven by opposite trends in the residual term, except in November and December when the long-term changes in the planetary wave forcing dominate. This is consistent with the fact that gravity wave driving is believed to dominate outside of the wintertime in the stratosphere, when the EP flux divergence is small (Fritts and Alexander, 2003). This underlines the considerable role of gravity waves in driving the B-D circulation and its long-term changes. This is on par with the findings of Li et al. (2008), McLandress and Shepherd (2009) and Butchart et al. (2010). For example, McLandress and Shepherd (2009) find that parameterized orographic gravity wave drag account for 40% of the long-term trend in annual mean net upward mass flux at 70 hPa.

While many studies rely solely on planetary waves to explain the stratospheric dynamics, this budget analysis draws attention to the need to account for gravity waves. As a result, a strong emphasis should be put on developing models with strong capabilities to accurately simulate gravity waves, both orographic and convectively forced. Finally, this study should be continued using various re-analysis dataset and assess the residual term calculated from the TEM momentum equation. There is also a clear need for a global dataset of gravity wave drag in the stratosphere for comparison purposes. There are many more issues that need to be addressed regarding long-term changes in the stratospheric dynamics. Since ozone depletion can directly alter planetary wave activity in the stratosphere through ozone photochemistry, ozone transport, and Newtonian cooling, there is a need for more theoretical and applied studies to investigate these mechanisms. Similarly, the impact of climate change due to increasing

ACPD
11, 11649–11690, 2011

anthropogenic emissions of greenhouse gas on the wave activity in the stratosphere needs to be better resolved.

Acknowledgements. The authors want to thank Terrence R. Nathan and R. Alan Plumb and the various anonymous reviewers for their comments. ERA-40 data were provided by the European Centre for Medium-Range Weather Forecasts from their website at http://data-portal.ecmwf.int/data/d/era40_daily/. This study was partially supported by the National Science Foundation grant ATM0733698.

References

Alexander, M. J. and Rosenlof, K. H.: Nonstationary gravity wave forcing of the stratospheric zonal mean wind, J. Geophys. Res., 101, 23465–23474, 1996. 11659, 11669

Alexander, M. J. and Rosenlof, K. H.: Gravity-wave forcing in the stratosphere: Observational constraints from the Upper Atmosphere Research Satellite and implications for parameterization in global models, J. Geophys. Res., 108, 4597, doi:10.1029/2003JD003373, 2003. 11659, 11660, 11669

Andrews, D. G., Mahlman, J. D., and Sinclair, R. W.: Eliassen-Palm Diagnostics of Wave-Mean Flow Interaction in the GFDL "SKYHI" General Circulation Model, J. Atmos. Sci., 40, 2768–2784, doi:10.1175/1520-0469(1983)040<2768:ETWATM>2.0.CO;2, 1983. 11652

Andrews, D. G., Holton, J. R., and Leovy, C. B.: Middle Atmosphere Dynamics, Academic Press, 489 pp., 1987. 11654, 11655, 11656, 11661

Baldwin, M. P. and Dunkerton, T. J.: Propagation of the Arctic Oscillation from the stratosphere to the troposphere, J. Geophys. Res., 104, 30937–30946, doi:10.1029/1999JD900445, 1999. 11651

Baldwin, M. P. and Dunkerton, T. J.: Stratospheric Harbingers of Anomalous Weather Regimes, Science, 294, 581–584, doi:10.1126/science.1063315, 2001. 11650, 11651

Baldwin, M. P., Gray, L. J., Dunkerton, T. J., Hamilton, K., Haynes, P. H., Randel, W. J., Holton, J. R., Alexander, M. J., Hirota, I., Horinouchi, T., Jones, D. B. A., Kinnersley, J. S., Marquardt,

ACPD
11, 11649–11690, 2011

Trends in forcing of stratospheric zonal-mean flow

E. Monier and B. C. Weare

C., Sato, K., and Takahashi, M.: The Quasi-Biennial Oscillation, Rev. Geophys., 39, 179–229, doi:10.1029/1999RG000073, 2001. 11665

Baldwin, M. P., Dameris, M., and Shepherd, T. G.: How will the stratosphere affect climate change?, Science, 316, 1576–1577, doi:10.1126/science.1144303, 2007. 11650

Black, R. X.: Stratospheric Forcing of Surface Climate in the Arctic Oscillation, J. Climate, 15, 268–277, doi:10.1175/1520-0442(2002)015<0268:SFOSCI>2.0.CO;2, 2002. 11651

Butchart, N., Scaife, A. A., Bourqui, M., de Grandpre, J., Hare, S. H. E., Kettleborough, J., Langematz, U., Manzini, E., Sassi, F., Shibata, K., Shindell, D., and Sigmond, M.: Simulations of anthropogenic change in the strength of the Brewer-Dobson circulation, Clim. Dyn., 27, 727–741, doi:10.1007/s00382-006-0162-4, 2006. 11666

Butchart, N., Cionni, I., Eyring, V., Shepherd, T. G., Waugh, D. W., Akiyoshi, H., Austin, J., Bruehl, C., Chipperfield, M. P., Cordero, E., Dameris, M., Deckert, R., Dhomse, S., Frith, S. M., Garcia, R. R., Gettelman, A., Giorgetta, M. A., Kinnison, D. E., Li, F., Mancini, E., McLandress, C., Pawson, S., Pitari, G., Plummer, D. A., Rozanov, E., Sassi, F., Scinocca, J. F., Shibata, K., Steil, B., and Tian, W.: Chemistry-Climate Model Simulations of Twenty-First Century Stratospheric Climate and Circulation Changes, J. Climate, 23, 5349–5374, doi:10.1175/2010JCLI3404.1, 2010. 11664, 11666, 11672

Callaghan, P. F. and Salby, M. L.: Three-Dimensionality and Forcing of the Brewer-Dobson Circulation, J. Atmos. Sci., 59, 976–991, doi:10.1175/1520-0469(2002)059<0976:TDAFOT>2.0.CO;2, 2002. 11655

Charney, J. G. and Drazin, P. G.: Propagation of Planetary-Scale Disturbances from the Lower into the Upper Atmosphere, J. Geophys. Res., 66, 83–109, doi:10.1029/JZ066i001p00083, 1961. 11657, 11662

Charney, J. G. and Eliassen, A.: A numerical method for predicting the perturbations of the middle latitude westerlies, Tellus, 1, 38–54, doi:10.1111/j.2153-3490.1949.tb01258.x, 1949. 11656

Chun, H. Y., Song, I. S., Baik, J. J., and Kim, Y. J.: Impact of a Convectively Forced Gravity Wave Drag Parameterization in NCAR CCM3, J. Climate, 17, 3530–3547, doi:10.1175/1520-0442(2004)017<3530:IOACFG>2.0.CO;2, 2004. 11660

Dunkerton, T.: On the Mean Meridional Mass Motions of the Stratosphere and Mesosphere, J. Atmos. Sci., 35, 2325–2333, doi:10.1175/1520-0469(1978)035<2325:OTMMMM>2.0.CO;2, 1978.

ACPD
11, 11649–11690, 2011

Dunkerton, T. J.: Annual variation of deseasonalized mean flow acceleration in the equatorial lower stratosphere, J. Meteor. Soc. Japan, 68, 499–508, 1990. 11655
Dunkerton, T. J.: The role of gravity waves in the quasi-biennial oscillation, J. Geophys. Res., 102, 26053–26076, 1997. 11665
Edmon Jr, H. J., Hoskins, B. J., and McIntyre, M. E.: Eliassen-Palm Cross Sections for the Troposphere, J. Atmos. Sci., 37, 2600–2616, doi:10.1175/1520-0469(1980)037<2600:EPCSFT>2.0.CO;2, 1980. 11660, 11669
Eichelberger, S. J. and Hartmann, D. L.: Changes in the strength of the Brewer-Dobson circulation in a simple AGCM, Geophys. Res. Lett., 32, L15 807, doi:10.1029/2005GL022924, 2005. 11662
Fritts, D. C. and Alexander, M. J.: Gravity wave dynamics and effects in the middle atmosphere, Rev. Geophys., 41, 1003, doi:10.1029/2001RG000106, 2003. 11655, 11666
Haklander, A. J., Siegmund, P. C., Sigmond, M., and Kelder, H. M.: How does the northern-winter wave driving of the Brewer-Dobson circulation increase in an enhanced-CO2 climate simulation?, Geophys. Res. Lett., 35, L07 702, doi:10.1029/2007GL033054, 2008. 11659, 11669, 11672
Hamilton, K.: Diagnostic Study of the Momentum Balance in the Northern Hemisphere Winter Stratosphere, Mon. Wea. Rev., 111, 1434–1441, 1983. 11666
Hartley, D. E., Villarin, J. T., Black, R. X., and Davis, C. A.: A new perspective on the dynamical link between the stratosphere and troposphere, Nature, 391, 471–474, doi:10.1038/35112, 1998. 11659, 11669
Hartmann, D. L.: The Dynamical Climatology of the Stratosphere in the Southern Hemisphere during Late Winter 1973, J. Atmos. Sci., 33, 1789–1802, 1976. 11651
Haynes, P.: Stratospheric Dynamics, Annu. Rev. Fluid Mech., 37, 263–293, doi:10.1146/annurev.fluid.37.061903.175710, 2005. 11659, 11669
Haynes, P. H., Marks, C. J., McIntyre, M. E., Shepherd, T. G., and Shine, K. P.: On the “Downward Control” of Extratropical Diabatic Circulations by Eddy-Induced Mean Zonal Forces, J. Atmos. Sci., 48, 651–679, 1991. 11650, 11661
Holton, J. R. and Wehrbein, W. M.: The Role of Forced Planetary Waves in the Annual Cycle of the Zonal Mean Circulation of the Middle Atmosphere, J. Atmos. Sci., 37, 1968–1983, doi:10.1175/1520-0469(1980)037<1968:TROFPW>2.0.CO;2, 1980. 11664
Hu, Y. and Tung, K. K.: Possible ozone-induced long-term changes in planetary wave activity in late winter, J. Climate, 16, 3027–3038, doi:10.1175/1520-

ACPD
11, 11649–11690, 2011

Trends in forcing of stratospheric zonal-mean flow

E. Monier and B. C. Weare

0442(2003)016<3027:POLCIP>2.0.CO;2, 2003. 11661

Ineson, S. and Scaife, A. A.: The role of the stratosphere in the European climate response to El Nino, Nat. Geosci., 2, 32–36, doi:10.1038/ngeo381, 2009. 11651, 11652, 11666, 11670

Iwasaki, T., Hamada, H., and Miyazaki, K.: Comparisons of Brewer-Dobson Circulations Diagnosed from Reanalyses, J. Meteor. Soc. Japan, 87, 997–1006, doi:10.2151/jmsj.87.997, 2009. 11651

Kanukhina, A. Y., Suvorova, E. V., Nechaeva, L. A., Skrygina, E. K., and Pogoreltsev, A. I.: Climatic variability of the mean flow and stationary planetary waves in the NCEP/NCAR reanalysis data, Ann. Geophys., 26, 1233–1241, doi:10.5194/angeo-26-1233-2008, 2008. 11661

Karpetchko, A. and Nikulin, G.: Influence of early winter upward wave activity flux on midwinter circulation in the stratosphere and troposphere, J. Climate, 17, 4443–4452, doi:10.1175/JCLI-3229.1, 2004. 11652, 11668

Karpetchko, A., Kyrö, E., and Knudsen, B. M.: Arctic and Antarctic polar vortices 1957–2002 as seen from the ERA-40 reanalyses, J. Geophys. Res., 110, D21 109, doi:10.1029/2005JD006113, 2005. 11651, 11652, 11670

Knudsen, B. M., Harris, N. R. P., Andersen, S. B., Christiansen, B., Larsen, N., Rex, M., and Naujokat, B.: Extrapolating future Arctic ozone losses, Atmos. Chem. Phys., 4, 1849–1856, doi:10.5194/acp-4-1849-2004, 2004. 11651, 11653, 11665

Kuroda, Y.: Role of the stratosphere on the predictability of medium-range weather forecast: A case study of winter 2003–2004, Geophys. Res. Lett., 35, L19 701, doi:10.1029/2008GL034902, 2008. 11653

Kuroda, Y. and Kodera, K.: Role of planetary waves in the stratosphere-troposphere coupled variability in the northern hemisphere winter, Geophys. Res. Lett., 26, 2375–2378, doi:10.1029/1999GL900507, 1999. 11651

Kuroda, Y. and Kodera, K.: Role of the Polar-night Jet Oscillation on the formation of the Arctic Oscillation in the Northern Hemisphere winter, J. Geophys. Res., 109, D11 112, doi:10.1029/2003JD004123, 2004. 11651

Lachlan-Cope, T. A., Connolley, W. M., and Turner, J.: The Role of the Non-Axisymmetric Antarctic Orography in forcing the Observed Pattern of Variability of the Antarctic Climate, Geophys. Res. Lett., 28, 4111–4114, doi:10.1029/2001GL013465, 2001. 11651

Li, F., Austin, J., and Wilson, J.: The strength of the Brewer-Dobson circulation in a changing climate: Coupled chemistry-climate model simulations, J. Climate, 21, 40–57,

doi:10.1175/2007JCLI1663.1, 2008. 11663
Limpasuvan, V., Hartmann, D. L., Thompson, D. W. J., Jeev, K., and Yung, Y. L.: Stratosphere-troposphere evolution during polar vortex intensification, J. Geophys. Res., 110, D24 101, doi:10.1029/2005JD006302, 2005. 11664, 11666, 11672
Lott, F. and Miller, M. J.: A new subgrid-scale orographic drag parametrization: Its formulation and testing, Quart. J. Roy. Meteor. Soc., 123, 101–127, doi:10.1002/qj.49712353704, 1997. 11651
Madden, R. A. and Labitzke, K.: A free Rossby wave in the troposphere and stratosphere during January 1979, J. Geophys. Res., 86, 1247–1254, doi:10.1029/JC086iC02p01247, 1981. 11659
McFarlane, N. A.: Gravity-Wave Drag, in: Numerical modeling of the global atmosphere in the climate system, edited by: Mote, P. and O'Neill, A., Kluwer Academic Publishers, Dordrecht, The Netherlands, 297–320, 2000. 11656
11659, 11660, 11669
McLandress, C.: On the importance of gravity waves in the middle atmosphere and their parameterization in general circulation models, J. Atmos. Sol.-Terr. Phys., 60, 1357–1383, 1998. 11661
McLandress, C. and Shepherd, T. G.: Simulated Anthropogenic Changes in the Brewer-Dobson Circulation, Including Its Extension to High Latitudes, J. Climate, 22, 1516–1540, doi:10.1175/2008JCLI2679.1, 2009. 11664, 11666, 11669, 11672
McWilliams, J. C.: Fundamentals of Geophysical Fluid Dynamics, Cambridge University Press, Cambridge, UK, 249 pp., 2006. 11656
Mieth, P., Grenfell, J. L., Langematz, U., and Kunze, M.: Sensitivity of the Freie Universitat Berlin Climate Middle Atmosphere Model (FUB-CMAM) to different gravity-wave drag parameterisations, Ann. Geophys., 22, 2693–2713, 2004. 11660
Miyazaki, K. and Iwasaki, T.: Diagnosis of meridional ozone transport based on mass-weighted isentropic zonal means, J. Atmos. Sci., 62, 1192–1208, doi:10.1175/JAS3394.1, 2005. 11655
Monier, E. and Weare, B. C.: Climatology and trends in the forcing of the stratospheric ozone transport, Atmos. Chem. Phys. Discuss., 11, 3693–3725, doi:10.5194/acpd-11-3693-2011, 2011. 11671
Nathan, T. R. and Cordero, E. C.: An ozone-modified refractive index for vertically propagating planetary waves, J. Geophys. Res., 112, D02 105, doi:10.1029/2006JD007357, 2007. 11671

Nikulin, G. and Karpechko, A.: The mean meridional circulation and midlatitude ozone buildup, Atmos. Chem. Phys., 5, 3159–3172, doi:10.5194/acp-5-3159-2005, 2005. 11655

Oort, A. H.: Global atmospheric circulation statistics, 1958–1973, Professional Paper 14, National Oceanic and Atmospheric Administration, Washington DC, 180 pp., 1983. 11656

Palmer, T. N.: Diagnostic Study of a Wavenumber-2 Stratospheric Sudden Warming in a Transformed Eulerian-Mean Formalism, J. Atmos. Sci., 38, 844–855, doi:10.1175/1520-0469(1981)038<0844:DSOAWS>2.0.CO;2, 1981. 11662

Palmer, T. N., Shutts, G. J., and Swinbank, R.: Alleviation of a systematic westerly bias in general circulation and numerical weather prediction models through an orographic gravity wave drag parametrization, Quart. J. Roy. Meteor. Soc., 112, 1001–1039, doi:10.1002/qj.49711247406, 1986. 11659, 11669

Parish, T. R., Bromwich, D. H., and Tzeng, R. Y.: On the role of the Antarctic continent in forcing large-scale circulations in the high southern latitudes, J. Atmos. Sci., 51, 3566–3579, doi:10.1175/1520-0469(1994)051<3566:OTROTA>2.0.CO;2, 1994. 11663

Pascoe, C. L., Gray, L. J., Crooks, S. A., Juckes, M. N., and Baldwin, M. P.: The quasi-biennial oscillation: Analysis using ERA-40 data, J. Geophys. Res., 110, D08 105, doi:10.1029/2004JD004941, 2005. 11653

Perlwitz, J. and Harnik, N.: Observational Evidence of a Stratospheric Influence on the Troposphere by Planetary Wave Reflection, J. Climate, 16, 3011–3026, doi:10.1175/1520-0442(2003)016<3011:OEOASI>2.0.CO;2, 2003. 11651

Pfeffer, R. L.: A Study of Eddy-induced Fluctuations of the Zonal-Mean Wind Using Conventional and Transformed Eulerian Diagnostics, J. Atmos. Sci., 49, 1036–1050, doi:10.1175/1520-0469(1992)049<1036:ASOEIF>2.0.CO;2, 1992. 11663

Randel, W. J., Udelhofen, P., Fleming, E., Geller, M., Gelman, M., Hamilton, K., D., K., Ortland, D., Pawson, S., Swinbank, R., Wu, F., Baldwin, M. P., Chanin, M. L., Keckhut, P., Labitzke, K., Remsberg, E., Simmons, A. J., and Wu, D.: The SPARC Intercomparison of Middle-Atmosphere Climatologies, J. Climate, 17, 986–1003, doi:10.1175/1520-0442(2004)017<0986:TSIOMC>2.0.CO;2, 2004. 11653

Randel, W. J., Garcia, R., and Wu, F.: Dynamical Balances and Tropical Stratospheric Upwelling, J. Atmos. Sci., 65, 3584–3595, doi:10.1175/2008JAS2756.1, 2008. 11661

Renwick, J. A.: Trends in the Southern Hemisphere polar vortex in NCEP and ECMWF reanalyses, Geophys. Res. Lett., 31, L07 209, doi:10.1029/2003GL019302, 2004. 11651, 11653, 11665, 11670

Richter, J. H., Sassi, F., Garcia, R. R., Matthes, K., and Fischer, C. A.: Dynamics of the middle atmosphere as simulated by the Whole Atmosphere Community Climate Model, version 3 (WACCM3), J. Geophys. Res., 113, D08 101, doi:10.1029/2007JD009269, 2008. 11660

Scaife, A. A., Butchart, N., Warner, C. D., and Swinbank, R.: Impact of a spectral gravity wave parameterization on the stratosphere in the met office unified model, J. Atmos. Sci., 59, 1473–1489, 2002. 11660, 11669

Schoeberl, M. R. and Strobel, D. F.: The Zonally Averaged Circulation of the Middle Atmosphere, J. Atmos. Sci., 35, 577–591, doi:10.1175/1520-0469(1978)035<0577:TZACOT>2.0.CO;2, 1978. 11661

Scinocca, J. F. and McFarlane, N. A.: The parametrization of drag induced by stratified flow over anisotropic orography, Quart. J. Roy. Meteor. Soc., 126, 2353–2393, 2000. 11659, 11660, 11669

Seol, D. I. and Yamazaki, K.: Residual mean meridional circulation in the stratosphere and upper troposphere: Climatological aspects, J. Meteor. Soc. Japan, 77, 985–996, 1999. 11661

Shepherd, T. G. and Shaw, T. A.: The Angular Momentum Constraint on Climate Sensitivity and Downward Influence in the Middle Atmosphere, J. Atmos. Sci., 61, 2899–2908, doi:10.1175/JAS-3295.1, 2004. 11661

Smith, A. K. and Lyjak, L. V.: An Observational Estimate of Gravity-Wave Drag From the Momentum Balance in the Middle Atmosphere, J. Geophys. Res., 90, 2233–2241, 1985. 11659, 11660, 11669

Song, Y. and Robinson, W. A.: Dynamical mechanisms for stratospheric influences on the troposphere, J. Atmos. Sci., 61, 1711–1725, doi:10.1175/1520-0469(2004)061<1711:DMFSIO>2.0.CO;2, 2004. 11651

Thompson, D. W. J. and Solomon, S.: Interpretation of recent Southern Hemisphere climate change, Science, 296, 895–899, doi:10.1126/science.1069270, 2002. 11651, 11665, 11670

Thompson, D. W. J. and Wallace, J. M.: Annular modes in the extratropical circulation. Part I: Month-to-month variability, J. Climate, 13, 1000–1016, doi:10.1175/1520-0442(2000)013<1000:AMITEC>2.0.CO;2, 2000. 11665

Uppala, S. M., Kallberg, P. W., Simmons, A. J., Andrae, U., Bechtold, V. D., Fiorino, M., Gibson, J. K., Haseler, J., Hernandez, A., Kelly, G. A., Li, X., Onogi, K., Saarinen, S., Sokka, N., Allan, R. P., Andersson, E., Arpe, K., Balmaseda, M. A., Beljaars, A. C. M., Van De Berg, L., Bidlot, J., Bormann, N., Caires, S., Chevallier, F., Dethof, A., Dragosavac, M., Fisher, M., Fuentes, M., Hagemann, S., Holm, E., Hoskins, B. J., Isaksen, L., Janssen, P. A. E. M., Jenne, R., McNally, A. P., Mahfouf, J. F., Morcrette, J. J., Rayner, N. A., Saunders, R. W., Simon, P., Sterl, A., Trenberth, K. E., Untch, A., Vasiljevic, D., Viterbo, P., and Woollen, J.: The ERA-40 re-analysis, Quart. J. Roy. Meteor. Soc., 131, 2961–3012, doi:10.1256/qj.04.176, 2005. 11653

van Noije, T. P. C., Eskes, H. J., van Weele, M., and van Velthoven, P. F. J.: Implications of the enhanced Brewer-Dobson circulation in European Centre for Medium-Range Weather Forecasts reanalysis ERA-40 for the stratosphere-troposphere exchange of ozone in global chemistry transport models, J. Geophys. Res., 109, D19 308, doi:10.1029/2004JD004586, 2004. 11653

Weare, B. C.: Dynamical modes associated with the Antarctic ozone hole, Atmos. Chem. Phys., 9, 5403–5416, doi:10.5194/acp-9-5403-2009, 2009. 11670

ACPD
11, 11649–11690, 2011

Trends in forcing of stratospheric zonal-mean flow

E. Monier and B. C. Weare

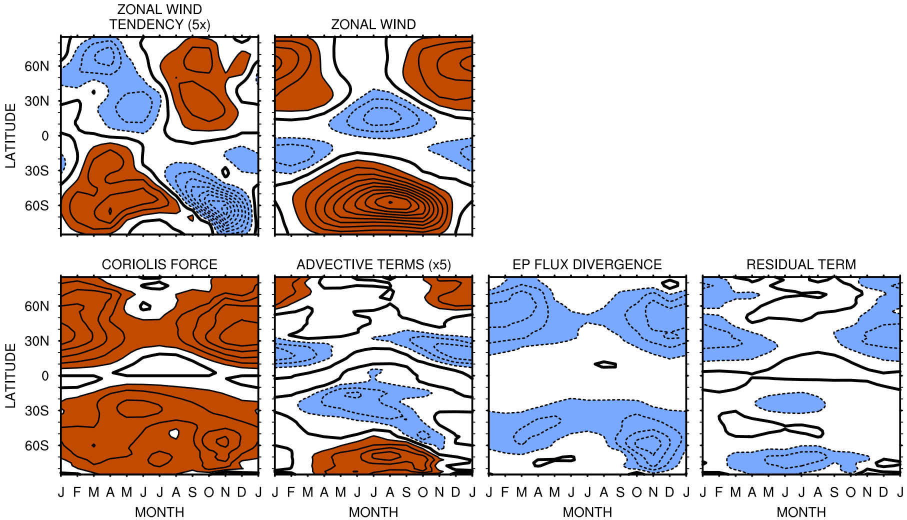

Fig. 1. Annual cycle of the stratospheric zonal wind, zonal wind tendency and each forcing term in the TEM momentum equation averaged between 100 and 10 hPa. Dashed (solid) lines and blue (brown) colors represent negative (positive) values while the bold solid line represent the zero-line. Contour spacing is 6 m s^{-1} for the zonal wind and 0.5 m s^{-1} day^{-1} for the zonal wind tendency. Note that the zonal wind tendency and advective terms are weak compared to the other terms and are therefore multiplied by 5.

ACPD
11, 11649–11690, 2011

E. Monier and B. C. Weare

Title Page
Abstract | Introduction
Conclusions | References
Tables | Figures
◀| |▶
◀ ▶
Back | Close
Full Screen / Esc
Printer-friendly Version
Interactive Discussion

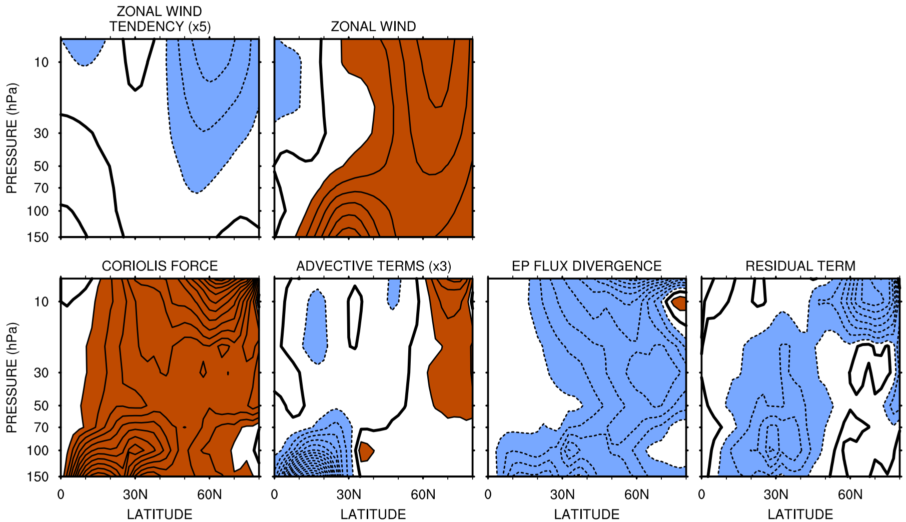

Fig. 2. Zonal-mean zonal wind, zonal wind tendency and its forcing terms in the NH averaged over JFM 1980–2001. Dashed (solid) lines and blue (brown) colors represent negative (positive) values while the bold solid line represent the zero-line. Contour interval is $0.5\,\mathrm{m\,s^{-1}\,day^{-1}}$ for the mean zonal wind tendency and the forcing terms and $6\,\mathrm{m\,s^{-1}}$ for the mean zonal wind. Note that the zonal wind tendency and advective terms are weak compared to the other terms and are therefore multiplied by respectively 5 and 3.

ACPD
11, 11649–11690, 2011

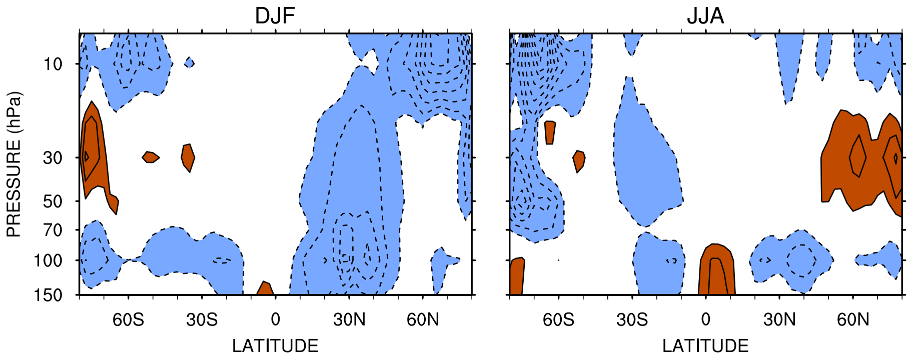

Fig. 3. Latitude-height cross-section of the residual term in the TEM momentum equation averaged of DJF and JJA. Dashed (solid) lines and blue (brown) colors represent negative (positive) values. Contour interval is 0.5 m s^{-1} day^{-1}.

ACPD
11, 11649–11690, 2011

Trends in forcing of stratospheric zonal-mean flow

E. Monier and B. C. Weare

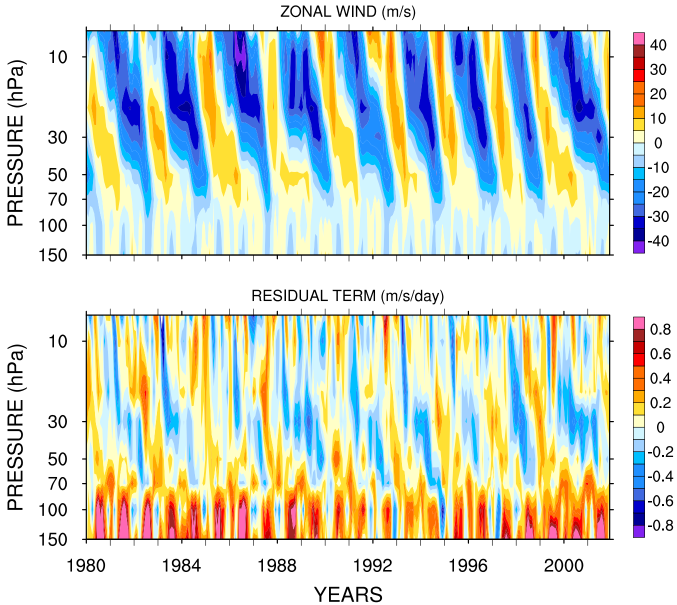

Fig. 4. Time series of the equatorial zonal-mean zonal wind ($\mathrm{m\,s^{-1}}$) and of the residual term ($\mathrm{m\,s^{-1}\,day^{-1}}$).

ACPD
11, 11649–11690, 2011

Trends in forcing of stratospheric zonal-mean flow

E. Monier and B. C. Weare

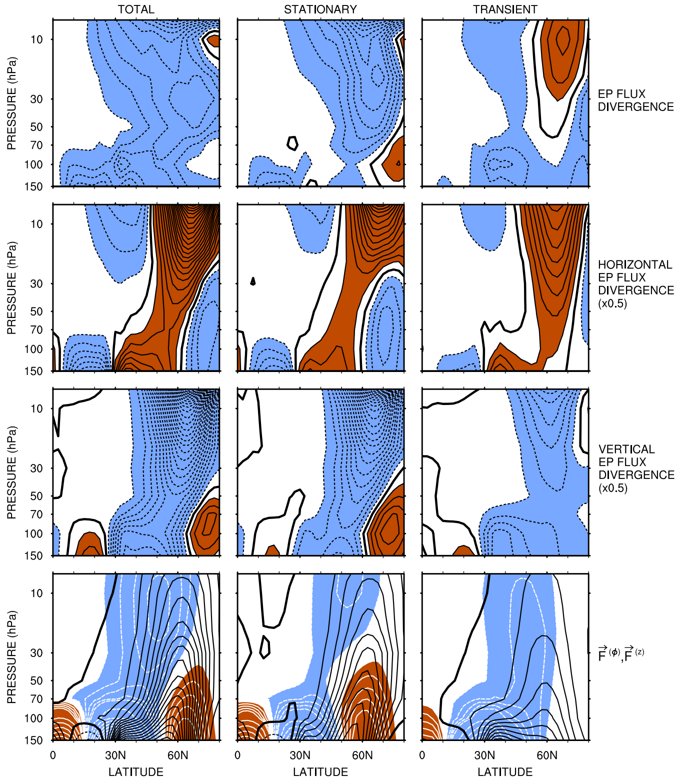

Fig. 5. Same as Fig. 2 but for the EP flux divergence, its horizontal and vertical components, and the EP flux vector, including stationary and transient components. Blue (brown) colors with dashed (solid) white lines represent negative (positive) values for $F^{(\phi)}$. Dashed (solid) black lines represent negative (positive) values while the bold solid line represent the zero-line for $F^{(z)}$. Contour spacing is $0.5\,\mathrm{m\,s^{-1}\,day^{-1}}$ for the EP flux divergence and its horizontal and vertical components, $10^6\,\mathrm{kg\,s^{-2}}$ for $F^{(\phi)}$ until $5\times10^6\,\mathrm{kg\,s^{-2}}$ and $5\times10^6\,\mathrm{kg\,s^{-2}}$ above, and $10^4\,\mathrm{kg\,s^{-2}}$ for $F^{(z)}$. Note that the horizontal and vertical components of the EP flux divergence are large compared to the EP flux divergence and are therefore multiplied by 0.5.

ACPD
11, 11649–11690, 2011

Trends in forcing of stratospheric zonal-mean flow

E. Monier and B. C. Weare

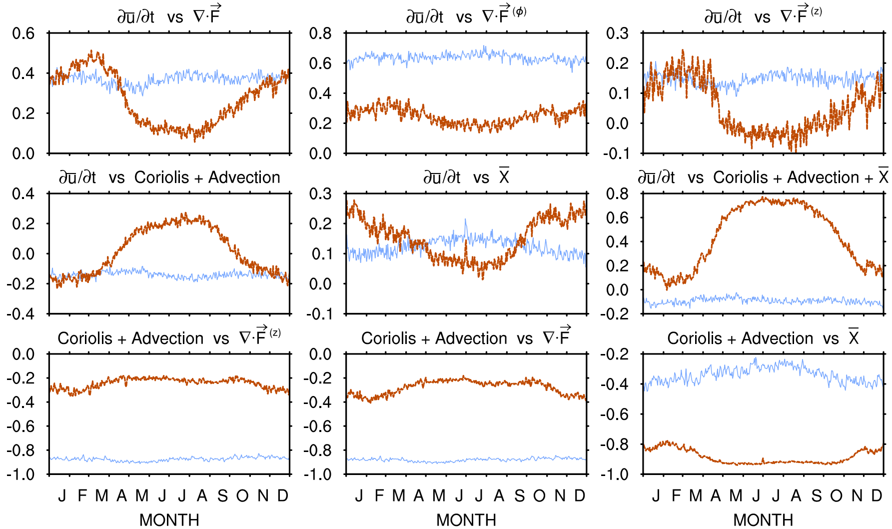

Fig. 6. Time variations of spatial correlations over the Northern Hemisphere in the troposphere (blue lines), up to 250 hPa, and in the stratosphere (brown lines), between 150 and 10 hPa, between the various terms of the TEM momentum equation. Correlation coefficients are calculated every 6 h over the time period 1 Jan 1980–31 Dec 2001.

ACPD
11, 11649–11690, 2011

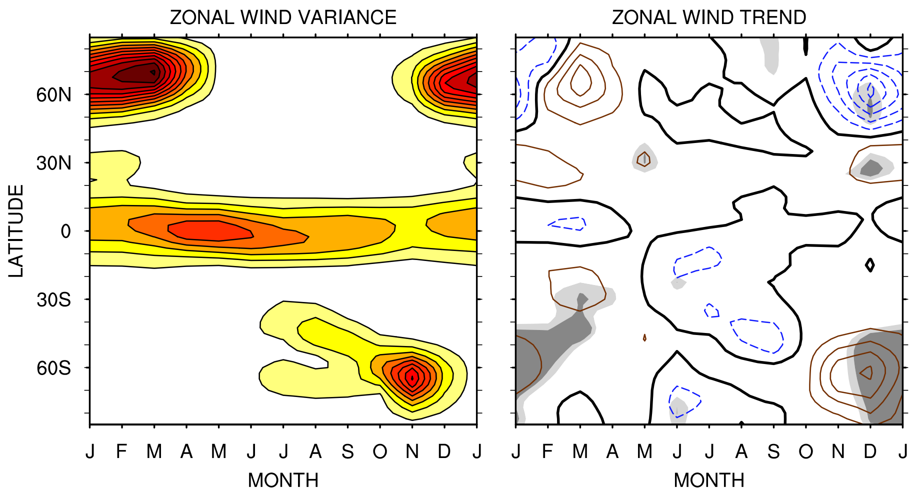

Fig. 7. Annual cycle of the zonal wind sample variance and trend. The variances and trends are calculated after the zonal wind is averaged between 100 and 10 hPa. Dashed blue (solid brown) lines represent negative (positive) values while the bold solid line represents the zero-line. Light grey (dark grey) shading represents the 90% (95%) statistical significance level of the trends. Contour spacing is 10 $m^2 s^{-2}$ for the variance and 1 $m s^{-1}$ per decade for the trend.

ACPD
11, 11649–11690, 2011

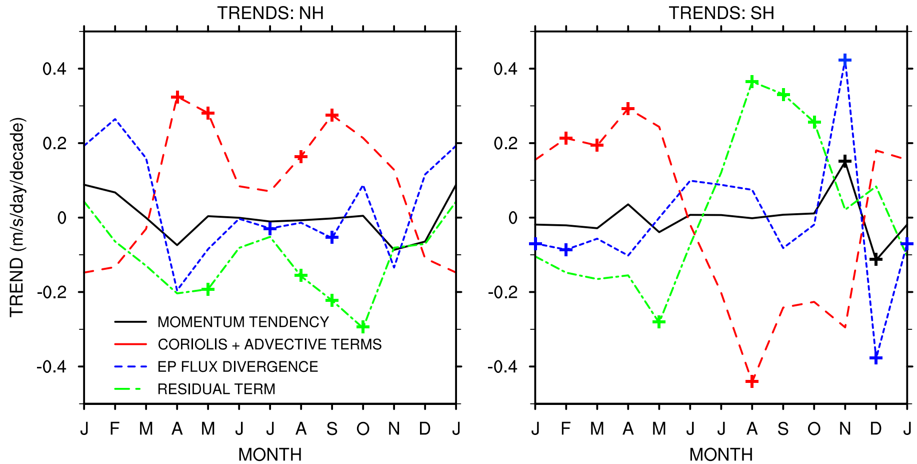

Fig. 8. Annual cycle of the trends in the momentum tendency and its forcing terms, for the (left) NH and the (right) SH. The trends are calculated after the momentum tendency and its forcing terms are averaged between 100 and 10 hPa and between 50°–70°. Trends that are statistically significant at the 95% level are indicated with a cross.

ACPD
11, 11649–11690, 2011

E. Monier and B. C. Weare

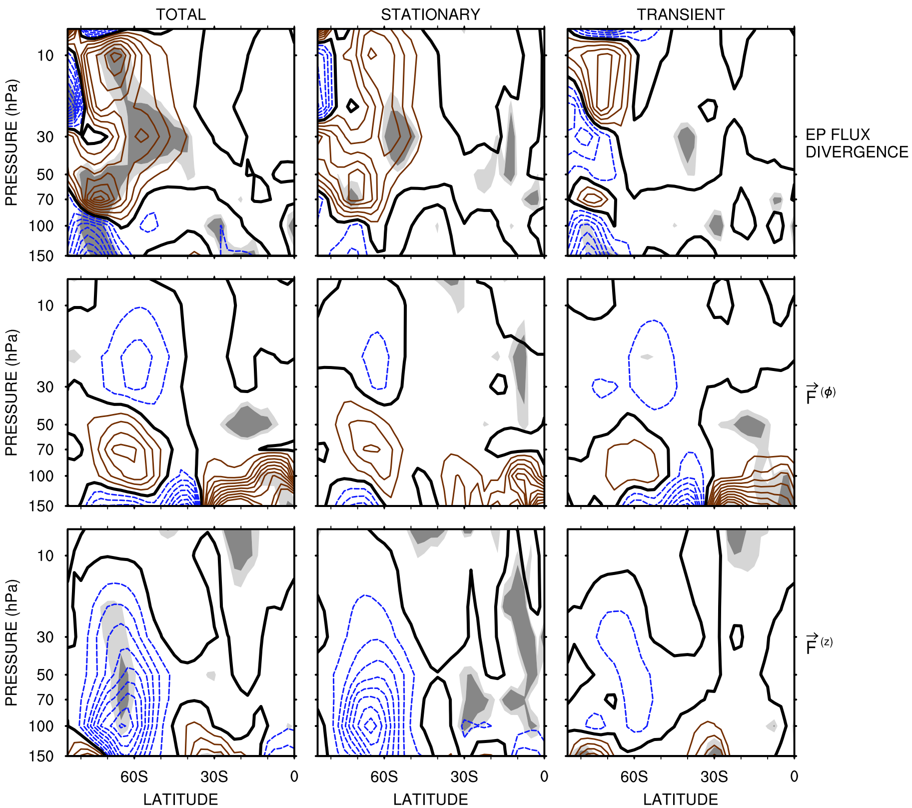

Fig. 9. Trends in the EP flux vector and its divergence, including stationary and transient components, for the month of November in the SH. Dashed (solid) lines represent negative (positive) values while the bold solid line represent the zero-line. Light grey (dark grey) shading represents the 90% (95%) statistical significance level of the trends. Contour spacing is $0.2\,\mathrm{m\,s^{-1}\,day^{-1}}$ per decade for the EP flux divergence, $2\times10^5\,\mathrm{kg\,s^{-2}}$ per decade for $\boldsymbol{F}^{(\phi)}$ and $2\times10^3\,\mathrm{kg\,s^{-2}}$ per decade for $\boldsymbol{F}^{(z)}$.

ACPD
11, 11649–11690, 2011

Trends in forcing of stratospheric zonal-mean flow

E. Monier and B. C. Weare

Title Page
Abstract | Introduction
Conclusions | References
Tables | Figures
◀| |▶
◀ ▶
Back | Close
Full Screen / Esc
Printer-friendly Version
Interactive Discussion

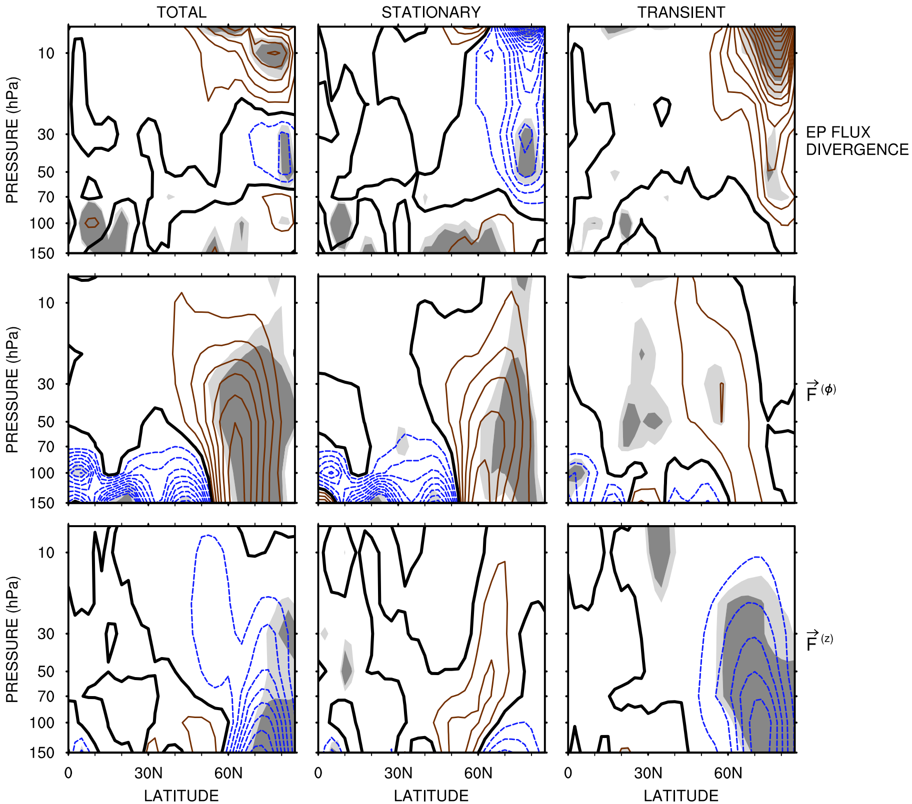

Fig. 10. Same as Fig. 9 but for the month of February in the NH. Contour spacing is $0.5\,\mathrm{m\,s^{-1}\,day^{-1}}$ per decade for the EP flux divergence, $5\times10^5\,\mathrm{kg\,s^{-2}}$ per decade for $F^{(\phi)}$ and $5\times10^3\,\mathrm{kg\,s^{-2}}$ per decade for $F^{(z)}$.

ACPD
11, 11649–11690, 2011

Trends in forcing of stratospheric zonal-mean flow

E. Monier and B. C. Weare